



Compositional grading in distributed Bragg reflectors, using discrete alloys, in vertical-cavity surface-emitting lasers

G.W. Pickrell^a, D.A. Louderback^a, M.A. Fish^a, J.J. Hindi^a, H.C. Lin^a,
M.C. Simpson^a, P.S. Guilfoyle^a, K.L. Lear^{b,*}

^a*OptiComp Corporation, 215 Elks Point Road, P.O. Box 10779, Zephyr Cove, NV 89448, USA*

^b*Electrical and Computer Engineering Department, Colorado State University, Fort Collins, CO 80523, USA*

Received 12 December 2004; accepted 11 March 2005

Available online 29 April 2005

Communicated by R.M. Biefeld

Abstract

We present experimental results on a technique for alloy composition grading within distributed Bragg reflectors (DBRs) for use in vertical-cavity, surface-emitting lasers (VCSELs). This technique, implemented using molecular beam epitaxy (MBE), employs multiple group-III sources, with different fluxes, to realize a set of $\text{Al}_x\text{Ga}_{1-x}\text{As}$ compositions without changing cell temperatures. By varying the source combination and layer thickness, different functional forms of compositional grading, such as linear and parabolic, can be closely approximated. This method, in combination with modulated doping profiles, was used to grow 980 nm VCSELs with low threshold currents, high output powers, and threshold voltages less than 1.45 V.

© 2005 Elsevier B.V. All rights reserved.

PACS: 81.15.Hi; 73.61.Ey

Keywords: A3. Molecular beam epitaxy; B2. Semiconducting III–V materials; B3. Distributed Bragg reflector; B3. Vertical-cavity surface-emitting laser (VCSEL)

1. Introduction

The popularity of vertical-cavity, surface-emitting lasers (VCSELs) for short-distance, data

communications has prompted many efforts to improve the performance of these devices. One area that has received substantial interest is in optimizing the electrical and optical properties of the distributed Bragg reflectors (DBRs) used as the VCSEL mirrors. The competing interests of both the optical and electrical requirements of the DBRs necessitates techniques such as alloy

*Corresponding author. Tel.: +970 4910718;
fax: +970 4912249.

E-mail address: klear@engr.colostate.edu (K.L. Lear).

compositional grading and modulated doping profiles within the layers in the mirror [1–4]. Utilizing these methods, high-performance VCSELs, at a variety of wavelengths, have been demonstrated using both metal-organic chemical vapor deposition (MOCVD) and molecular beam epitaxy (MBE). Using MOCVD, researchers have employed analog grading schemes, by varying the flow-rate of the group-III source, to smoothly grade the alloy composition between the mirror pairs [5]. Alternatively, MBE researchers have employed digital alloys, consisting of thin layers of AlAs and GaAs with a varying duty cycle, to compositionally grade the DBR materials [1]. Additionally, analog compositional grading schemes have been realized utilizing MBE by changing effusion cell temperatures between mirror layers to affect a change in composition [6]. MBE growth techniques have disadvantages including degradation in shutter mechanisms due to the high number of shutter actuations and a reduction in reproducibility due to inaccuracies in changing cell temperatures. We present an MBE growth technique, employing a set of discrete $\text{Al}_x\text{Ga}_{1-x}\text{As}$ alloys, that allows for effective compositional grading with a reduced number of shutter actuations for each effusion cell and without changing cell temperatures during device growth. Applying this novel technique, VCSELs operating at a wavelength near 980 nm have been fabricated with low threshold currents and voltages. It is important to note that these VCSELs were developed for applications requiring robust performance over a large range of operating conditions. These devices were not specifically designed to achieve minimized threshold characteristics.

2. Description of growth method

The devices described in this letter were grown using a Veeco Applied Epi Gen III MBE growth system. The Gen III system has 12 available source ports on the growth chamber allowing for the use of redundant group-III sources, thus enabling novel growth techniques. The source configuration in these experiments consisted of three aluminum

(Al) sources, two gallium (Ga) sources, one indium (In) source, a valved arsenic (As) cracking source, a silicon (Si) dopant source, and a carbon tetrabromide (CBr_4) dopant source. Through proper choice of growth rates for the multiple Al and Ga effusion cells, different combinations of sources can be employed to achieve over 20 different $\text{Al}_x\text{Ga}_{1-x}\text{As}$ compositions without changing any cell temperatures.

Selection of the growth rates was constrained by several factors including total growth rate, alloy composition, and the magnitude of the change in composition between each alloy. To insure high-quality material and reproducible structures, the growth rates were kept below 3 monolayers per second (ML/s). The alloy compositions needed for flexible DBR design included Al-mole fractions ranging from 0 to 0.9 with minimal changes in composition between the available alloys. Based on these constraints, the growth rates chosen included: $\text{Al}_1 = 0.7$ ML/s, $\text{Al}_2 = 0.4$ ML/s, $\text{Al}_3 = 0.2$ ML/s, $\text{Ga}_1 = 1.3$ ML/s, and $\text{Ga}_2 = 0.2$ ML/s. Simply changing the state of the shutter for different sources can quickly change the alloy composition of adjacent layers. For example, a combination of $\text{Al}_1 + \text{Al}_3 + \text{Ga}_1$ gives an Al composition of 41%. Closing the Al_3 shutter lowers the Al composition to 35%.

Since the alloy composition for each combination of sources is fixed, an additional degree of freedom for design is allowed by changing the layer thickness within the DBR grading. Using this technique, a linear grading scheme was designed for the n-type DBR, while a uniparabolic grading scheme [12] was used for the p-type DBR. Fig. 1(a) shows the design for a linear grade between GaAs and $\text{Al}_{0.87}\text{Ga}_{0.13}\text{As}$ layers within a DBR period. The linear grade was distributed over a thickness of 16 nm using seven intermediate alloy compositions. The thickness of each of the discrete grading layers ranged from 1.7 to 2.3 nm. As Fig. 1(a) shows, the desired continuous compositional profile is closely approximated by a series of thin, discrete layers, each with a different $\text{Al}_x\text{Ga}_{1-x}\text{As}$ alloy composition and thickness. Similarly, Fig. 1(b) shows a uniparabolic grade between GaAs and $\text{Al}_{0.87}\text{Ga}_{0.13}\text{As}$ layers. The parabolic grade was distributed over a thickness of 22 nm using

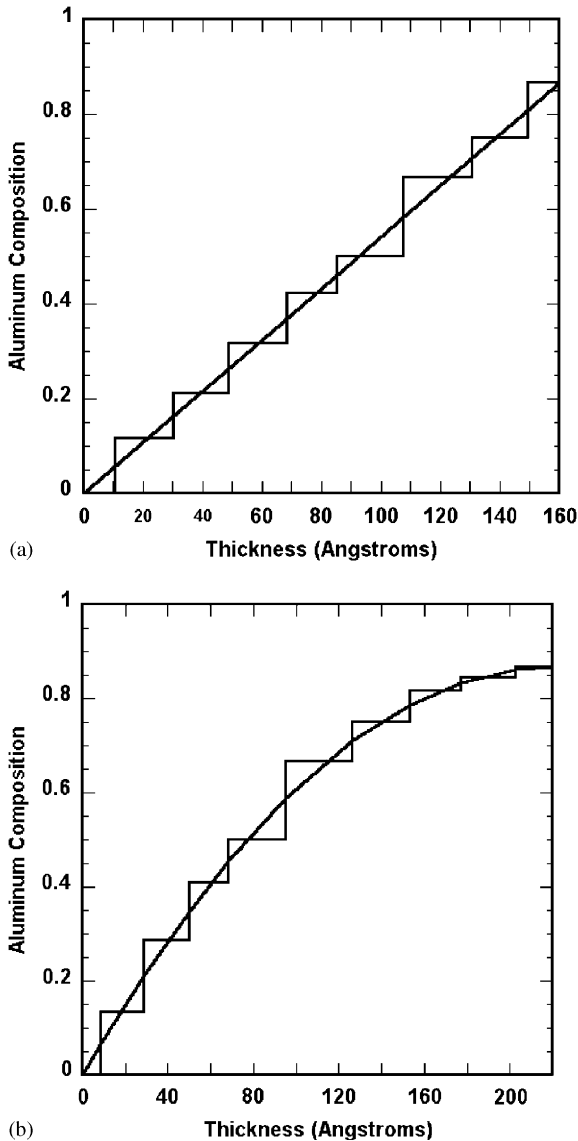


Fig. 1. Aluminum composition vs. thickness for (a) a linear grading scheme and (b) a parabolic grading scheme realized using discrete alloys. The figures show the compositions used for grading between a GaAs layer and an $\text{Al}_{0.87}\text{Ga}_{0.13}\text{As}$ layer within a DBR. For clarity, a smooth line was included to represent the desired continuous compositional profile of the compositional grade.

eight intermediate alloy compositions. For this grading scheme, the thickness of the discrete grading layers ranged from 1.9 to 3.1 nm. For

comparison, the desired continuous compositional profiles of the grades are included in the figure.

3. Device structure

A VCSEL was grown to verify the device design and modeling efforts. The VCSEL structure was grown on a three-inch, n-type (100) GaAs substrate. The device structure consisted of a 30.5 pair, n-type, GaAs/ $\text{Al}_{0.87}\text{Ga}_{0.13}\text{As}$ DBR grown using the linear grading scheme described above. The first 25 pairs of the DBR were Si-doped at a level of $3 \times 10^{18} \text{ cm}^{-3}$. To achieve this doping level in the GaAs and $\text{Al}_{0.87}\text{Ga}_{0.13}\text{As}$ layers, the temperature of the Si cell was ramped during the compositional grade. Over the next two DBR periods, the doping level in the DBR was lowered to $7 \times 10^{17} \text{ cm}^{-3}$ in the GaAs layer and $1 \times 10^{18} \text{ cm}^{-3}$ in the $\text{Al}_{0.87}\text{Ga}_{0.13}\text{As}$ layer, holding these doping levels constant for the remainder of the n-type DBR. Next, a $1-\lambda$ cavity, including $\text{Al}_{0.32}\text{Ga}_{0.68}\text{As}$ separate confinement heterostructure layers and three, 8 nm $\text{In}_{0.2}\text{Ga}_{0.8}\text{As}$ quantum wells with 8 nm GaAs barriers was grown.

The VCSEL's p-type DBR was grown using the parabolic grading scheme described above and included 18 pairs. The first p-type DBR period contained a 40 nm $\text{Al}_{0.98}\text{Ga}_{0.02}\text{As}$ layer for use as an oxide aperture. The doping level of the five p-type DBR layers nearest the cavity was $1 \times 10^{18} \text{ cm}^{-3}$ in the $\text{Al}_{0.87}\text{Ga}_{0.13}\text{As}$ layer and $7 \times 10^{17} \text{ cm}^{-3}$ in the GaAs layers. Within the parabolic grades, the doping was modulated to selectively place a high concentration of dopants at the null of the optical field and to minimize the dopants where the optical field was high [7]. While varying the composition from GaAs to $\text{Al}_{0.87}\text{Ga}_{0.13}\text{As}$, the doping levels within the graded region varied from 8×10^{17} to $2.3 \times 10^{18} \text{ cm}^{-3}$. When grading the composition from $\text{Al}_{0.87}\text{Ga}_{0.13}\text{As}$ toward GaAs, the doping level in the graded region ranged from 3×10^{18} to $4 \times 10^{18} \text{ cm}^{-3}$. During the first 13.5 nm of the GaAs layer, the doping was kept at $4 \times 10^{18} \text{ cm}^{-3}$ to aid in flattening the valence band [8]. To offset the accumulation of holes at the heterointerface of the GaAs to $\text{Al}_{0.87}\text{Ga}_{0.13}\text{As}$ transition, a 7 nm

GaAs layer, doped with Si at a concentration of $2 \times 10^{18} \text{ cm}^{-3}$, was used at the GaAs/Al_{0.87}Ga_{0.13}As interface [7]. The next 12 p-type DBR pairs were doped at a higher level: $2.1 \times 10^{18} \text{ cm}^{-3}$ for the GaAs layers and $3 \times 10^{18} \text{ cm}^{-3}$ for the Al_{0.87}Ga_{0.13}As layers. The same modulated doping profiles were used in the parabolically graded regions in the highly doped DBR layers. The structure was completed with a DBR period containing a GaAs contact layer, doped at a concentration of $1 \times 10^{19} \text{ cm}^{-3}$.

4. Modeling of compositional grades

The equilibrium band diagrams of the mirror grades were simulated from the alloy composition profiles shown in Fig. 1 using the dopant type and concentration profiles detailed above. The simulations were performed using SimWindows [9], a one-dimensional semiconductor heterostructure modeling tool self-consistently solving the electric field distribution and carrier concentrations based on Fermi–Dirac statistics. Equilibrium calculations provide useful indications of the energetic barriers in low-resistance heterostructures where minimal voltage drops do not significantly perturb the equilibrium field distribution.

The resulting equilibrium band diagrams for the highly doped, n-type mirror and p-type mirrors are shown in Fig. 2(a) and (b), respectively. The linear change of Al-composition translated to a linear change in energy within the n-type graded regions. The maximum energy change of the conduction band edge within the DBR was 135 meV using this design. In the p-type mirror, smaller energy differences in the valence band edge were seen. The maximum energy change of the valence band edge within the DBR was approximately 60 meV for this design. Considering that most of a VCSEL's resistance is typically caused by the p-type mirror, these simulations were promising for use in devices.

5. Device results

Using standard fabrication procedures, top-emitting VCSELs were processed for characteriza-

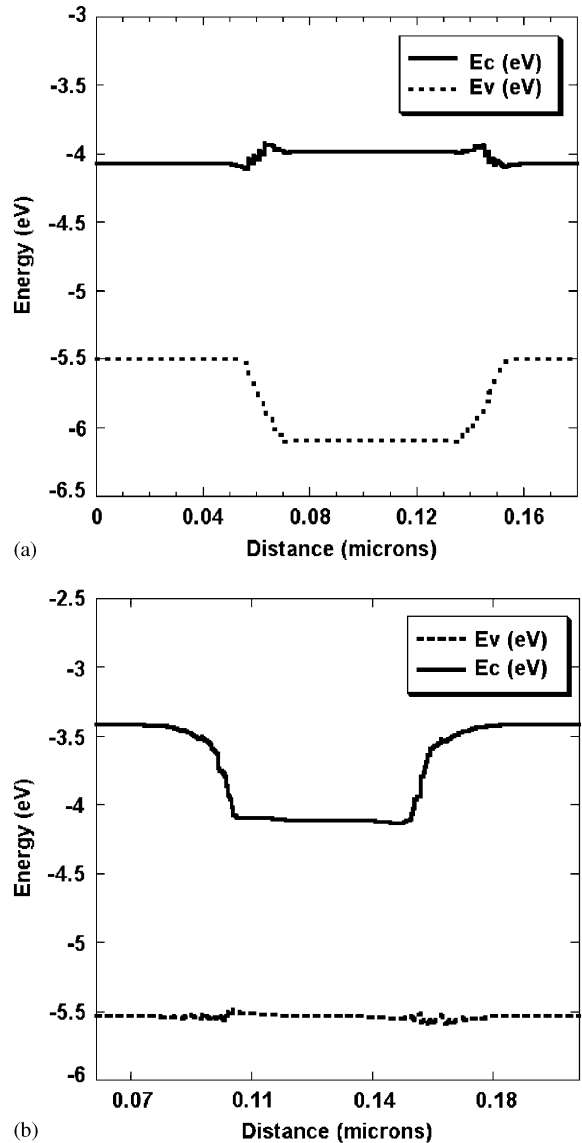


Fig. 2. Equilibrium energy band diagrams, including the conduction and valence bands, for (a) the linear grading scheme used in the n-type DBR, and (b) the parabolic grading scheme used in the p-type DBR. The figures include both the upward and downward compositional grades within the DBR.

tion. Devices with various aperture diameters were fabricated and characterized using an electrical probing test station with a stage temperature of 20 °C and a photodetector placed over the top of the device to collect the laser emission. Fig. 3

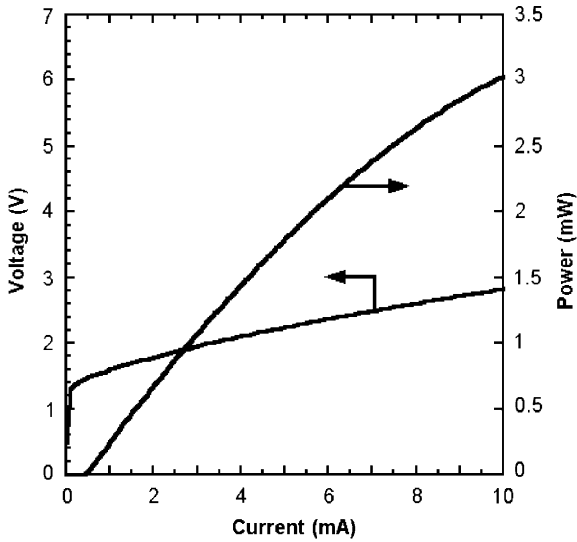


Fig. 3. Light-current-voltage characteristics of a 980 nm VCSEL, with an oxide aperture diameter of $4.5\ \mu\text{m}$, fabricated using the discrete compositional grading method. The threshold current for this device was $394\ \mu\text{A}$, and the threshold voltage was $1.456\ \text{V}$.

shows a typical light-current-voltage (LIV) plot for a VCSEL with an aperture diameter of $4.5\ \mu\text{m}$. The threshold current for this device was $394\ \mu\text{A}$ with a threshold voltage of $1.456\ \text{V}$ (including measurement equipment resistance). At a bias current of $10\ \text{mA}$, this device emitted more than $3\ \text{mW}$ of power. Single-mode VCSELs, with $3\ \mu\text{m}$ aperture diameters, had threshold currents as low as $200\ \mu\text{A}$. Multimode devices, with $5\ \mu\text{m}$ aperture diameters, exhibited threshold voltages of $1.449\ \text{V}$. These device results show similar operating characteristics to published results. For example, multimode devices grown with continuously graded DBRs, via MOCVD, demonstrated threshold voltages of significantly less than $2\ \text{V}$ [10]. In addition, oxide-apertured devices, grown using MBE, demonstrated similar threshold voltage of significantly less than $2\ \text{V}$ [11]. The device characteristics demonstrated in this study indicate that this compositional-grading technique provides an effective alternative to conventional DBR grading methods and results in high-performance devices with low threshold currents and voltages, as well as multi-milliwatt output powers.

6. Conclusions

An MBE growth method, using multiple group-III sources, was demonstrated to grade $\text{Al}_x\text{-Ga}_{1-x}\text{As}$ alloy compositions between layers in a DBR. Through different source combinations, growth rates, and layer thickness, linear and parabolic grading schemes were designed for use in a VCSEL. Using a modulated doping scheme, a linearly graded n-type DBR and a parabolically graded p-type mirror, $980\ \text{nm}$ VCSELs with low threshold currents and voltages, and high output powers were demonstrated. Typical multimode devices showed threshold voltages of approximately $1.45\ \text{V}$, threshold currents of less than $500\ \mu\text{A}$, and output powers of $3\ \text{mW}$. With this design, the lowest threshold voltage was determined to be $1.449\ \text{V}$ including the resistance of the measurement equipment, and the lowest threshold current measured was $200\ \mu\text{A}$. These device characteristics indicate that this growth technique is suitable for the fabrication of high-performance VCSELs for a variety of applications.

Acknowledgements

This work was supported in part by the Missile Defense Agency (MDA), the Naval Air Systems Command (NAVAIR), and the Air Force Research Laboratory (AFRL).

References

- [1] K. Tai, L. Yang, Y.H. Wang, J.D. Wynn, A.Y. Cho, *Appl. Phys. Lett.* 56 (1990) 2496.
- [2] P. Zhou, J. Cheng, C.F. Schaus, S.Z. Sun, K. Zheng, E. Armour, C. Hains, W. Hsin, D.R. Myers, G.A. Vawter, *IEEE Photon. Technol. Lett.* 3 (1991) 591.
- [3] S.A. Chalmers, K.L. Lear, K.P. Killeen, *Appl. Phys. Lett.* 62 (1993) 1585.
- [4] M.G. Peters, B.J. Thibeault, D.B. Young, J.W. Scott, F.H. Peters, A.C. Gossard, L.A. Coldren, *Appl. Phys. Lett.* 63 (1993) 3411.
- [5] P. Zhou, J. Cheng, C.F. Schaus, S.Z. Sun, D. Kopchik, C. Hains, W. Hsin, C. Chen, D.R. Myers, G.A. Vawter, G.R. Olbright, R.P. Bryan, *IEEE Trans. Electron Devices* 38 (1991) 2697.
- [6] M. Hong, D. Vakhshoori, J.P. Mannaerts, Y.F. Hsieh, *J. Vac. Sci. Technol. B* 13 (1995) 758.

- [7] E.R. Hegblom, N.M. Margalit, A. Fiore, L.A. Coldren, *Electron. Lett.* 34 (1998) 895.
- [8] D.I. Babić, G.H. Döhler, J.E. Bowers, E.L. Hu, *IEEE J. Quantum Electron.* 33 (1997) 2195.
- [9] D.W. Winston, R.E. Hayes, *IEEE J. Quantum Electron.* 34 (1998) 707.
- [10] B. Lu, P. Zhou, J. Cheng, K. Malloy, J. Zolper, *Appl. Phys. Lett.* 65 (1994) 1337.
- [11] D.A. Louderbach, Ph. D. Dissertation, University of California, 2003.
- [12] K.L. Lear, R.P. Schneider, *Appl. Phys. Lett.* 68 (1996) 605.